Eur. J. Biochem. **270**, 1025–1032 (2003) © FEBS 2003 doi:10.1046/j.1432-1033.2003.03478.x

Biosynthesis of riboflavin in Archaea

6,7-Dimethyl-8-ribityllumazine synthase of *Methanococcus jannaschii*

Ilka Haase[1], Simone Mörtl[1], Peter Köhler[2], Adelbert Bacher[1] and Markus Fischer[1]

[1]*Lehrstuhl für Organische Chemie und Biochemie, Technische Universität München, Garching, Germany;*
[2]*Deutsche Forschungsanstalt für Lebensmittelchemie, Lichtenbergstr. 4, D-85747 Garching, Germany*

Heterologous expression of the putative open reading frame MJ0303 of *Methanococcus jannaschii* provided a recombinant protein catalysing the formation of the riboflavin precursor, 6,7-dimethyl-8-ribityllumazine, by condensation of 5-amino-6-ribitylamino-2,4(1*H*,3*H*)-pyrimidinedione and 3,4-dihydroxy-2-butanone 4-phosphate. Steady state kinetic analysis at 37 °C and pH 7.0 indicated a catalytic rate of 11 nmol·mg^{-1}·min^{-1}; K_m values for 5-amino-6-ribitylamino-2,4(1*H*,3*H*)-pyrimidinedione and 3,4-dihydroxybutanone 4-phosphate were 12.5 and 52 μM, respectively. The enzyme sediments at an apparent velocity of about 12 S. Sedimentation equilibrium analysis indicated a molecular mass around 1 MDa but was hampered by nonideal solute behaviour. Negative-stained electron micrographs showed predominantly spherical particles with a diameter of about 150 Å. The data suggest that the enzyme from *M. jannaschii* can form capsids with icosahedral 532 symmetry consisting of 60 subunits.

Keywords: Archaea; *Methanococcus jannaschii*; riboflavin biosynthesis; lumazine synthase; quaternary structure.

Flavocoenzymes derived from riboflavin (vitamin B_2) (structure 6, Fig. 1) serve as essential redox cofactors in all cells. Whereas the biosynthesis of the vitamin has been studied in considerable detail in eubacteria and yeasts (reviewed in [1–3]), little is known about its formation in Archaea. The initial step of riboflavin biosynthesis in eubacteria, fungi and plants has been shown to involve the formation of 2,5-diamino-5-ribosylamino-4(3*H*)-pyrimidinone 5′-phosphate from GTP (structure 1) by the hydrolytic release of formate and pyrophosphate catalysed by GTP cyclohydrolase II [4,5] (Fig. 1). The enzyme product is converted to 5-amino-6-ribitylamino-2,4(1*H*,3*H*)-pyrimidinedione (structure 2) by a sequence of deamination, side chain reduction and dephosphorylation [6–9]. Deamination and reduction proceed in reverse order in eubacteria and yeasts [8]; the enzyme responsible for dephosphorylation has still not been identified.

Condensation of 5-amino-6-ribitylamino-2,4(1*H*,3*H*)-pyrimidinedione (structure 2) with 3,4-dihydroxy-2-butanone 4-phosphate (structure 4) is catalysed by 6,7-dimethyl-8-ribityllumazine synthase (lumazine synthase). This enzyme has been isolated from eubacteria, yeasts and plants [10–17]. The carbohydrate substrate, 3,4-dihydroxy-2-butanone 4-phosphate (structure 4), is obtained from ribulose 5-phosphate (structure 3) by a complex skeletal rearrangement catalysed by 3,4-dihydroxy-2-butanone 4-phosphate synthase, which has been found in eubacteria, fungi and plants [9,18–20]. The final step in the biosynthesis of riboflavin (structure 6) is the dismutation of 6,7-dimethyl-8-ribityllumazine (structure 5) affording 5-amino-6-ribitylamino-2,4(1*H*,3*H*)-pyrimidinedione (structure 2) as a second product which is recycled by lumazine synthase [21–26].

The biosynthesis of riboflavin in Archaea is incompletely understood. *In vivo* experiments with *Methanobacterium thermoautotrophicum* using ^{13}C-labeled acetate showed that the xylene ring of the vitamin is assembled from two four-carbon fragments, in correspondence with earlier findings in eubacteria and eukaryotes [27]. 5-Amino-6-ribitylamino-2,4(1*H*,3*H*)-pyrimidinedione (structure 2) was shown subsequently to serve as a precursor for both riboflavin (structure 6) and 5-deaza-7-hydroxyriboflavin (structure 7), the chromophore of coenzyme F_{420} in *M. thermoautotrophicum* [27]. More recent work identified a riboflavin synthase of *M. thermoautotrophicum* that has relatively little sequence similarity with riboflavin synthases of eubacteria, fungi and plants [28]. Recently, the open reading frame MJ0671 of *Methanococcus jannaschii* was shown to specify an enzyme catalysing the reduction of 2,5-diamino-6-ribosylamino-4(3*H*)-pyrimidinone 5′-phosphate [29].

This paper shows that the hypothetical open reading frame MJ0303 of *M. jannaschii* specifies a lumazine synthase that is structurally similar to orthologs from eubacteria and eukaryots.

Correspondence to M. Fischer, Lehrstuhl für Organische Chemie und Biochemie, Technische Universität München, Lichtenbergstr. 4, D-85747 Garching, Germany.
Fax: + 49 89 289 13363; Tel.: + 49 89 289 13336;
E-mail: markus.fischer@ch.tum.de
(Received 14 November 2002, revised 20 January 2003, accepted 23 January 2003)

Experimental procedures

Materials

5-Amino-6-ribitylamino-2,4(1*H*,3*H*)-pyrimidinedione (structure 2) was freshly prepared from 5-nitro-6-ribitylamino-2,

4(1*H*,3*H*)-pyrimidinedione [30,31] by catalytic hydrogenation [32]. 3,4-Dihydroxy-2-butanone 4-phosphate (structure 4) was freshly prepared from ribose 5-phosphate by treatment with pentose phosphate isomerase and 3,4-dihydroxy-2-butanone 4-phosphate synthase [19]. Recombinant 3,4-dihydroxy-2-butanone 4-phosphate synthase of *Escherichia coli* was prepared using published procedures [33]. Oligonucleotides were custom-synthesized by MWG Biotech, Ebersberg, Germany.

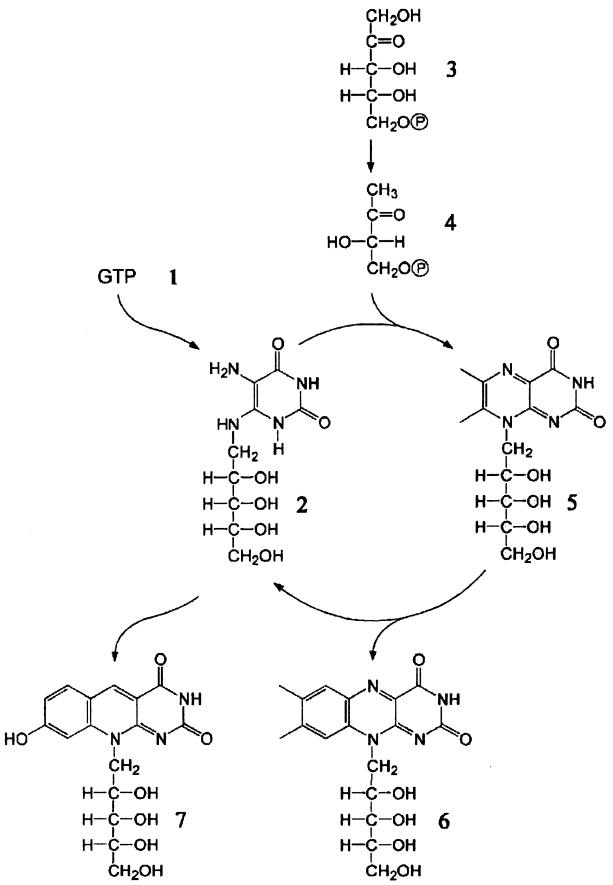

Fig. 1. Terminal reactions in the pathway of riboflavin biosynthesis.

Bacterial strains

Microbial strains and plasmids used in this study are summarized in Table 1.

Construction of an expression plasmid

PCR amplification using *M. jannaschii* cDNA as a template and the oligonucleotides, MJ-RibE-1 and MJ-RibE-2 (Table 2) as primers produced a DNA fragment that served as a template for a second round of PCR amplification using the oligonucleotides, MJ-RibE-2 and MJ-RibE-3 as primers. The resulting product was purified with the purification kit from Qiagen, digested with the restriction endonucleases *Eco*RI and *Bam*HI, and ligated into the expression-vector pNCO113 (Table 1) [34] digested with the same enzymes. The resulting plasmid, pNCO-MJ-RibE, was transformed into *Escherichia coli* XL1-Blue cells (Table 1) [35].

Construction of an expression plasmid for modified lumazine synthase of *Bacillus subtilis*

The coding region of the *ribH* gene of *B. subtilis* was amplified by PCR using the plasmid, p602-BS-RibH [36] as the template and the oligonucleotides, BS-RibH-ΔN-G6 and BS-RibH-2 as primers (Table 2). The resulting product was cleaved with the restriction enzymes *Eco*RI and *Bam*HI and ligated into the plasmid, pNCO113 (Table 1) that had been treated with the same enzymes. The resulting plasmid,

Table 1. Bacterial strains and plasmids.

Strain or plasmid	Relevant characteristics	Source
E. coli strain XL-1-Blue	*recA1, endA1, gyrA96, thi-1, hsdR17, supE44, relA1, lac[F′, proAB, lacI^{q}ZΔM15, Tn10(tet^r)]*	[35]
Plasmids for the RibE gene of *M. jannaschii* and the RibH gene of *B. subtilis*	Expression vector	[34]
pNCO113	Expression vector	[34]
pNCO-MJ-RibE	RibE gene wild type	This study
pNCO-BS-RibH-ΔN-G6	RibH gene truncated at the N-terminus	This study

Table 2. Oligonucleotides used for construction of expression plasmids. Recognition sites are emboldened.

Designation	Endonuclease	Sequence
MJ-RibE-1		5′-GGAGAAATTAACCATGGTATTGATGGTAAATCTTGG-3′
MJ-RibE-2	*Bam*HI	5′-TTCTTTGGAAG**GGATCC**AATTTCATAAAAATTT-3′
MJ-RibE-3	*Eco*RI	5′-ACACA**GAATTC**ATTAAAGAGGAGAAATTAACTATG-3′
BS-RibH-ΔN-G6	*Eco*RI, *Nco*I	5′-ATAATAGAA**GAATTC**ATTAAAGAGGAGAAATTAA**CCATGGG**AAATTTAGTTGGTACAG-3′
BS-RibH-2	*Bam*HI	5′-TATTAT**GGATTC**TTATTCGAAAGAACGGTTTAAG-3′

pNCO-RibH-ΔN-G6, was transformed into *E. coli* XL1-Blue cells.

DNA sequencing

Sequencing was performed by the dideoxy chain termination method [37] using a model 377A DNA sequencer from Applied Biosystems (Foster City, CA, UK). Plasmid DNA was isolated from cultures (5 mL) of XL-1 Blue strains grown overnight in LB medium containing ampicillin (150 mg·L^{-1}) using Nucleobond AX20 columns (Macherey und Nagel, Düren, Germany).

Purification of *M. jannaschii* 6,7-dimethyl-8-ribityllumazine synthase

The frozen cell mass of the recombinant *E. coli* strain XL1-Blue carrying the plasmid, pNCO-MJ-RibE, was thawed in 20 mM potassium phosphate, pH 7.0. The suspension was ultrasonically treated and centrifuged. The supernatant was placed on a column of hydroxyapatite (2.5 × 10 cm, Amersham Pharmacia Biotech, Freiburg, Germany) that had been equilibrated with 20 mM potassium phosphate, pH 7.1. The column was developed with a linear gradient of 0.02–1 M potassium phosphate, pH 7.1 (total volume, 400 mL). Fractions were combined and ammonium sulfate was added to a final concentration of 2.46 M. The precipitate was harvested and dissolved in 100 mM potassium phosphate, pH 7.0. The solution was placed on top of a Sephacryl S-400 column (2.6 × 60 cm, Amersham Pharmacia Biotech, Freiburg, Germany) which was developed with 100 mM potassium phosphate, pH 7.0. Fractions were combined and concentrated by ultrafiltration.

Purification of the lumazine synthases of *B. subtilis* and *A. aeolicus*

Purification of the mutant enzyme of *B. subtilis* and the wildtype lumazine synthase of *A. aeolicus* was performed as described [17,38].

SDS/PAGE

SDS/PAGE using 16% polyacrylamide gels was performed as described [39]. Molecular mass standards were supplied by Sigma.

Peptide sequencing

Sequence determination was performed by the automated Edman method using a 471-A Protein Sequencer (Perkin Elmer).

Assay of 6,7-dimethyl-8-ribityllumazine synthase activity

Reaction mixtures contained 100 mM potassium phosphate, pH 7.0, 5 mM EDTA, 5-amino-6-ribitylamino-2,4(1*H*,3*H*)-pyrimidinedione (structure 2, Fig. 1) (freshly prepared) and 3,4-dihydroxy-2-butanone 4-phosphate (structure 4) as required, and protein. The reaction was monitored photometrically at 410 nm.

Analytical ultracentrifugation

Experiments were performed with an analytical ultracentrifuge Optima XL-A from Beckman Instruments equipped with absorbance optics. Aluminum double sector cells equipped with quartz windows were used throughout. Protein solutions were dialysed against 50 mM potassium phosphate, pH 7.0. The partial specific volume was estimated from the aminoacid composition yielding a value of 0.752 mL·g^{-1} [40].

Electron microscopy

Carbon-coated copper grids were exposed to a glow discharge. They were covered with a drop of protein solution (about 1 mg·mL^{-1}) for 2 min and rinsed repeatedly with 2% uranyl acetate and distilled water. They were finally soaked with 2% uranyl acetate for 90 s and blotted dry with filter paper. Electron micrographs were obtained with a JEOL-JEM-100CX Microscope on Imago-EM 23 electron microscopy films.

Electrospray mass spectrometry

Experiments were performed as described by Mann and Wilm [41] using a triple quadrupol ion spray mass spectrometer API365 (SciEx, Thornhill, Ontario, Canada).

Results

The putative open reading frame MJ0303 of *M. jannaschii* specifying 141 amino acid residues shows ≈26% identity with lumazine synthase of *B. subtilis*. The *M. jannaschii* open reading frame was amplified by PCR and was placed under the control of a T5 promoter and *lac* operator in the expression plasmid pNCO113. A recombinant *E. coli* strain carrying that plasmid expressed a 16-kDa protein as judged by SDS gel electrophoresis.

The recombinant protein was purified by a sequence of two chromatographic procedures. Electrospray mass spectroscopy afforded a subunit molecular mass of 15645 Da; an exact match with the predicted mass. Edman degradation of the N-terminus afforded the sequence MVLMVNLGFV in agreement with the translated open reading frame.

The recombinant protein catalyses the formation of 6,7-dimethyl-8-ribityllumazine (structure 5) from 5-amino-6-ribitylamino-2,4(1*H*,3*H*)-pyrimidinedione (structure 2) and L-3,4-dihydroxy-2-butanone 4-phosphate (structure 4). Steady state kinetic measurements at 37 °C and pH 7.0 gave a V_{max} value of 11 nmol·mg^{-1}·min^{-1} and K_m values of 12.5 μM for 5-amino-6-ribitylamino-2,4(1*H*,3*H*)-pyrimidinedione (structure 2) and 52 μM for 3,4-dihydroxy-2-butanone 4-phosphate (structure 4) (Table 3).

The substrates of lumazine synthase can react spontaneously under formation of 6,7-dimethyl-8-ribityllumazine in the absence of any catalyst [42]. All kinetic experiments reported in this paper involved control samples without enzyme in order to correct for any contributions of the nonenzymatic reaction.

The catalytic rates of lumazine synthases from typical mesophilic bacteria and fungi such as *E. coli*, *B. subtilis*, *Saccharomyces cerevisiae* and *Schizosaccharomyces pombe*,

Table 3. Properties of lumazine synthases.

Origin	K_m 1[a] (μM)	K_m 2[b] (μM)	V_{max} (37 °C) (nmol mg^{-1}·min^{-1})	Sedimentation velocity (S)	Source
M. jannaschii	52	12.5	11	~ 12	This study
A. aeolicus	26	10.0	31	–	This study
B. subtilis	55	9.0	242	26.5	[47]
E. coli	62	4.2	197	26.8	[14]
S. cerevisiae	90	4.0	257	5.5	[14]
S. pombe	67	5.0	217	5.0	[48]
S. oleracea	26	20.0	275	–	[49]

[a] K_m for 3,4-dihydroxy-2-butanone 4-phosphate, [b] K_m for 5-amino-6-ribitylamino-2,4(1*H*,3*H*)-pyrimidinedione.

are in the range of 200–250 nmol·mg^{-1}·min^{-1} (Table 3). The catalytic activity of lumazine synthase from spinach at 37 °C is 275 nmol·mg^{-1} min^{-1}. Not surprisingly, the catalytic activity of enzyme from the thermophilic archaeon at 37 °C is low in comparison with mesophilic organisms. At a temperature of 70 °C, the catalytic rate of the enzyme is 90 nmol·mg^{-1}·min^{-1}. Steady state kinetic experiments in the temperature range of 10–80 °C gave a linear Arrhenius Plot with a E_A of 63.7 kJ·mol^{-1} and an Arrhenius constant of $A = 2.9 \times 10^8$ s^{-1} (Fig. 2, Table 4).

Sedimentation equilibrium analysis of *M jannaschii* produced an approximate mass of 1.1 MDa suggesting an icosahedral 60-mer structure analogous to those found in *B. subtilis*, *A. aeolicus* and spinach, but the deviations of the experimental data from the calculated sedimentation profile of an ideal solute (residuals in the top part of Fig. 3) are relatively large. This could be explained by nonideal solute behaviour or by an equilibrium state involving different oligomeric forms.

Electron micrographs of negative-stained lumazine synthase of *M. jannaschii* show roughly spherical particles with diameters around 15 nm (Fig. 4C). The images of the particles resemble closely those of icosahedral lumazine synthases from *B. subtilis*, *E. coli* and *A. aeolicus* (Fig. 4A,B,D). It should be noted that smaller oligomers, if present, are likely to have less characteristic shapes and may elude detection in electron micrographs.

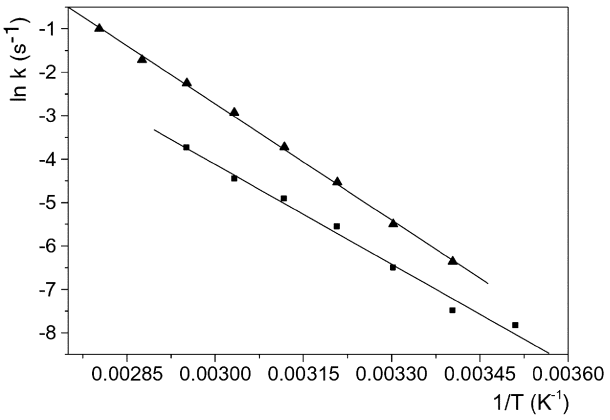

Fig. 2. Arrhenius plots for the rate catalysed by lumazine synthase of *M. jannaschii* (■) and *A. aeolicus* (▲). Natural log of the steady state rate in s^{-1} vs. the inverse of the temperature (in Kelvin).

Compared with the lumazine synthase from *B. subtilis*, the enzyme from *M. jannaschii* has a shortened N-terminus (Fig. 5). In the lumazine synthase of *B. subtilis*, the first six amino acid residues form a β-strand contact with the central β-sheet of an adjacent subunit which was considered to be important for the association of the icosahedron. In order to prove the importance of the N-terminal sequence in the *B. subtilis* enzyme an N-terminal deletion mutant was produced as described in the Experimental procedures section. The mutant protein failed to fold in a soluble conformation when more than five amino acid residues were removed from the N-terminal domain (data not shown).

Boundary sedimentation of lumazine synthase from *M. jannaschii* afforded a sedimentation constant of about 12 S, whereas the sedimentation constants of 60-meric icosahedral lumazine synthases from various other organisms were invariably found in the range of 26 S (Table 3). Notably, the sedimenting boundary of the *M. jannaschii* enzyme is broader than that expected for a monodisperse, ideal solute. It is therefore not possible to determine the sedimentation rate with high accuracy.

In order to illustrate the characteristic difference in the sedimentation behaviour of the enzymes from *M. jannaschii* and *B. subtilis*, Fig. 6 shows a boundary sedimentation experiment with a mixture of the two proteins. In the upper part of that figure, the *B. subtilis* enzyme is seen to sediment as a relatively sharp boundary with an apparent velocity of 26 S. By comparison, the *M. jannaschii* enzyme observed in the lower part is characterized by a relatively slow-sedimenting, broad boundary.

Discussion

Lumazine synthase of the thermophilic Archaea show only relatively low similarity with those of eubacteria (Figs 5 and 7). In negatively stained electron micrographs, the enzyme from *M. jannaschii*, *E. coli*, *A. aeolicus* and *B. subtilis* all appear as essentially spherical particles with diameters around 15 nm (Fig. 4) [43]. In sedimentation equilibrium studies, these proteins have apparent molecular masses of 0.9–1 MDa, which identifies them as homo-oligomeric aggregates. However, the sedimentation equilibrium data of the *M. jannaschii* enzyme deviate significantly from the prediction for a homodisperse solute with ideal solute behaviour (Fig. 3).

The enzymes from *B. subtilis*, *A. aeolicus*, and spinach have all been shown by X-ray crystallography to consist

Table 4. Activation parameters for lumazine synthases from different organisms.

Origin	E_a (kJ mol^{-1})	ΔG (kJ mol^{-1})	ΔH (kJ mol^{-1})	ΔS (J K^{-1}·mol^{-1})	Source
M. jannaschii	63.7 ± 3.1	91 ± 6.6	61 ± 3.1	−96.8 ± 10.1	This study
B. subtilis	74.6 ± 1.1	83 ± 1.0	76 ± 1.0	−22.4 ± 3.6	[50]
A. aeolicus	74.3 ± 1.1	88 ± 2.3	72 ± 1.1	−53.8 ± 3.4	This study
S. oleracea	87.1 ± 1.7	82 ± 0.4	84 ± 1.7	7.0 ± 5.6	[51]
M. grisea	90.0 ± 2.9	80 ± 0.4	83 ± 2.9	9.8 ± 9.8	[51]
E. coli	87.9 ± 4.2	82 ± 0.4	85 ± 4.2	9.8 ± 14.0	[51]
Uncatalysed	46.3 ± 0.6	83 ± 0.5	45 ± 0.5	−127.1 ± 1.6	[50]

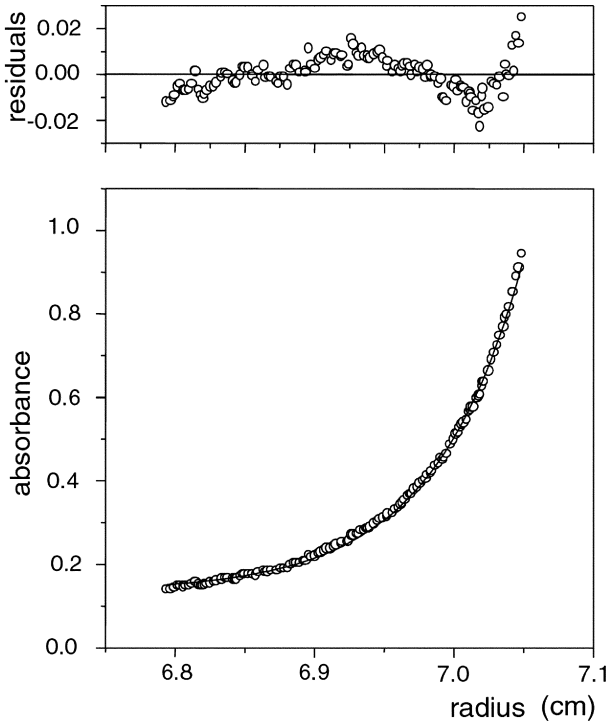

Fig. 3. Sedimentation equilibrium centrifugation of lumazine synthase from *M. jannaschii*. A solution containing 0.3 mg protein per mL of 50 mM potassium phosphate, pH 7.0, was centrifuged at 2000 ***g*** and 4 °C for 72 h. The line was calculated for an ideal solute with a relative mass of about 1 MDa and a partial specific volume of 0.752 mL·g^{-1}. Residuals are shown in the top section.

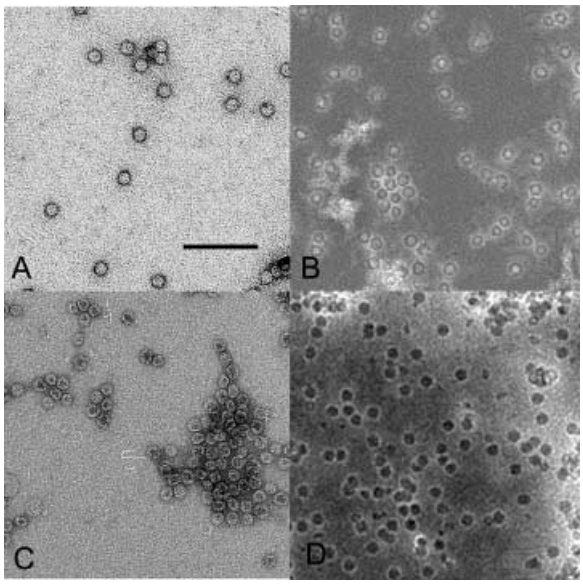

Fig. 4. Electron micrographs of recombinant lumazine synthases from *B. subtilis* (A), *E. coli* (B), *M. jannaschii* (C) and *A. aeolicus* (D). The proteins were adsorbed on carbon and negatively stained with uranyl acetate. The bars represent 100 nm.

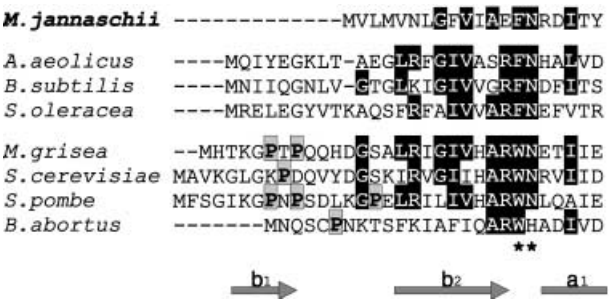

Fig. 5. Sequence comparison of the N-terminal domains of lumazine synthases. Conserved residues are shown with inverted contrast. Prolines are shown in grey. Residues that are part of the active site are marked by an asterisk [16].

of 60 identical subunits [15–17]. The particles have icosahedral 532 symmetry and form approximately spherical capsids with a central, approximately spherical cavity with a diameter of about 5 nm. In the case of lumazine synthase from Bacillaceae, the capsids can enclose a homotrimeric riboflavin synthase module [12,16,44,45]. That enzyme complex can catalyse both terminal reaction steps of the riboflavin biosynthesis, thus producing riboflavin from one molecule of structure 2 and two molecules of structure 4. The unusual molecular topology of that enzyme complex is associated with kinetic anomalies resulting from substrate channeling between the different protein modules [46].

Whereas the electron microscopic observations and the sedimentation equilibrium data suggest a similar molecular structure (i.e., a 60-meric icosahedral capsid architecture) for the *M. jannaschii* enzyme, the boundary sedimentation data are at odds with that model. The icosahedral lumazine synthases of *E. coli* and *B. subtilis* all sediment at a rate of about 26 S and show close to ideal solute behaviour. In

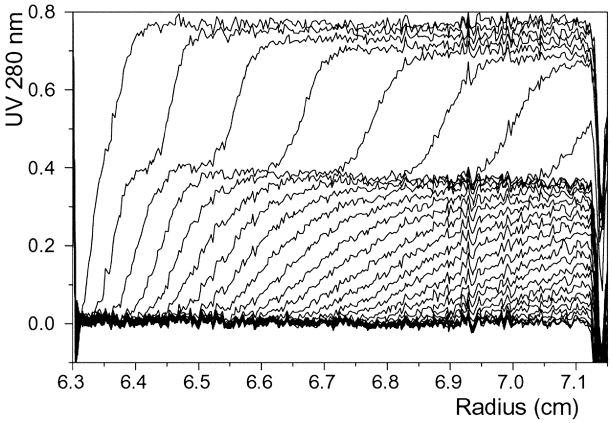

Fig. 6. Boundary sedimentation. A mixture of 0.5 mg of each of the lumazine synthase from *B. subtilis* and *M. jannaschii* (per mL of 50 mM potassium phosphate, pH 7.0) was centrifuged at 160 000 ***g*** and 20 °C. Protein concentration was monitored photometrically at 280 nm.

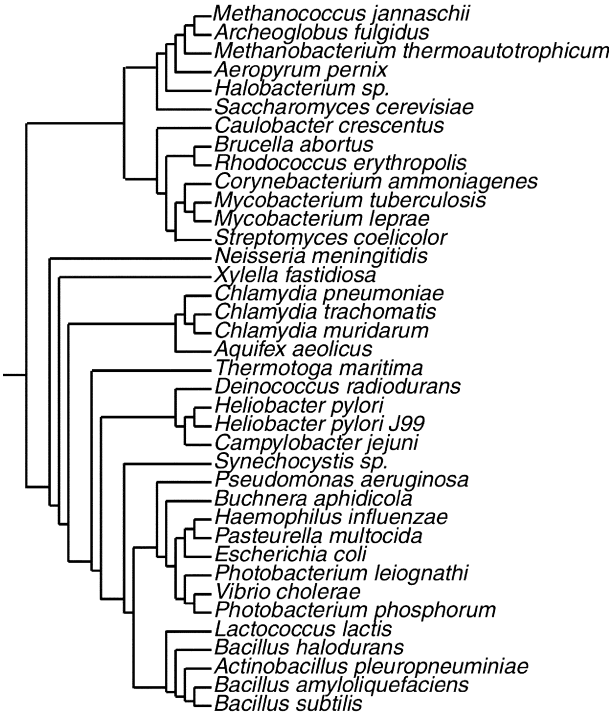

Fig. 7. Phylogenetic tree of microbial lumazine synthases.

contrast, the *M. jannaschii* enzyme sediments as an overly broad boundary with components ranging from 11–13 S. On closer inspection, the presence of heterogeneous components sedimenting at substantially higher resp. lower velocities is also found. This apparent molecular heterogeneity is not due to the presence of impurities; the recombinant enzyme appears pure as judged by electrophoresis under denaturating conditions and by mass spectrometry. Thus, the unexpected sedimentation behaviour is believed to reflect molecular heterogeneity at the quaternary structure level which is at present not understood. A more detailed description of structural peculiarities of the *M. jannaschii* enzyme may have to await the determination of its three-dimensional structure by X-ray crystallography.

It is unknown whether the *M. jannaschii* enzyme associates with a different protein, similar to the riboflavin synthase–lumazine synthase complex of Bacillaceae.

The kinetic properties of the *M. jannaschii* are remarkably different from those of the orthologs of eubacteria and eukaryots. At 37 °C, the catalytic rate is only about 5% when compared to mesophilic enzymes (Table 3). Even at a temperature of 70 °C, the specific activity is relatively low, with a value of 90 nmol·mg^{-1}·min^{-1}. By comparison, lumazine synthase from the hyperthermophilic, *A. aeolicus*, has catalytic rates of 31 and 425 nmol·mg^{-1}·min^{-1} at temperatures of 37 and 70 °C (Fig. 2, Table 3).

The activation parameters of the *M. jannaschii* enzyme are strikingly different from those reported for other lumazine synthases. Enzymes from eubacteria and eukaryotes have activation energies ranging from about 74–90 kJ·mol^{-1}, more than 10 kJ·mol^{-1} in excess of the value for the enzyme from *M. jannaschii* (Table 4). On the other hand, the *M. jannaschii* enzyme has a large negative activation entropy (–97 J·K^{-1}·mol^{-1}), whereas the activation entropies of the other enzymes in Table 4 are close to zero, except for *A. aeolicus*.

The folding topology of all lumazine synthase studied at atomic resolution is characterized by parallel β-sheets flanked on both sides by α-helices. The N-terminus typically participates in the β-sheet of the adjacent subunit. The N-terminal part of the *M. jannaschii* enzyme is significantly shorter as compared to the orthologs from eubacteria, fungi and plants and could hardly serve as a link to the β-sheet of the adjacent subunit (Fig. 5). Remarkably, the pentameric lumazine synthase of *S. cerevisiae* tolerates the deletion of 17 amino acid residues at the N-terminus [13]. On the other hand, the icosahedral lumazine synthase of *B. subtilis* fails to fold correctly when more than five amino acid residues are deleted of the N-terminus. It is also noteworthy that the N-terminal segments of the pentameric, but not those of the icosahedral lumazine synthases, comprise proline residues. The *M. jannaschii* enzyme differs from both groups of lumazine synthases with respect to the N-terminus and the sedimentation behaviour.

Coenzyme biosynthesis pathways need to produce only relatively small amounts of the final product. Although the excess production of riboflavin has been observed in certain ascomycetes such as *Ashbya gossypii* and *Eremothicum ashbyii*, the amount of riboflavin produced by most microorganisms and by plants is low. The production of excess amounts could reduce the overall fitness by the wasting of resources. Hence, it is not surprising that the enzymes of riboflavin biosynthesis typically have low catalytic activities – in the low nmol·mg^{-1}·min^{-1} range. These low activities may reflect the virtual absence of selective pressure conducive to the evolution of more efficient catalysis. This is particularly striking in case of the reaction catalysed by lumazine synthase which has been found to proceed with remarkably high velocity in mM substrate mixtures at pH 7.0 and room temperature [47]. The acceleration of that reaction by lumazine synthase from

M. jannaschii is unimpressive at best, with a catalytic rate in the range of 11 nmol·mg^{-1}·min^{-1} corresponding to a turnover number of around 0.17 per enzyme subunit per minute. In light of these arguments, the complex molecular structures of many well-studied lumazine synthases appears even more remarkable. Apparently, an amazingly complex molecular machinery is required in order to achieve the slight catalytic acceleration in the formation of 6,7-dimethyl-8-ribityllumazine that suits the metabolic requirements of the microorganisms.

Acknowledgements

We thank K. O. Stetter for providing chromosomal DNA from *M. jannaschii*, Richard Feicht and Lars Schulte for skillfull assistance and Angelika Werner for help with the preparation of the manuscript. This work was supported by grants from the Deutsche Forschungsgemeinschaft and the Fonds der Chemischen Industrie.

References

1. Young, D.W. (1986) The biosynthesis of the vitamins thiamin, riboflavin, and folic acid. *Nat. Prod. Report* **3**, 395–419.
2. Bacher, A., Eberhardt, S. & Richter, G. (1996) Biosynthesis of riboflavin. In Escherichia *and* Salmonella (Neidhardt, F.C., Ingraham, J.L., Low, K.B., Magasanik, B., Schaechter, M. & Umbarger, H.E., eds), pp. 657–664, American. Society for Microbiology, Washington, DC.
3. Bacher, A., Eberhardt, S., Eisenreich, W., Fischer, M., Herz, S., Illarionov, B., Kis, K. & Richter, G. (2001) Biosynthesis of riboflavin. *Vitam. Horm.* **61**, 1–49.
4. Foor, F. & Brown, G.M. (1975) Purification and properties of guanosine triphosphate cyclohydrolase II from *Escherichia coli*. *J. Biol. Chem.* **250**, 3545–3551.
5. Foor, F. & Brown, G.M. (1980) GTP-cyclohydrolase II from *Escherichia coli*. *Metods Enzymol.* **66**, 303–307.
6. Burrows, R.B. & Brown, G.M. (1978) Presence in *Escherichia coli* of a deaminase and a reductase involved in biosynthesis of riboflavin. *J. Bacteriol.* **136**, 657–667.
7. Hollander, I. & Brown, G.M. (1979) Biosynthesis of riboflavin: reductase and deaminase of *Ashbya gossypii*. *Biochem. Biophys. Res. Commun.* **89**, 759–763.
8. Nielsen, P. & Bacher, A. (1981) Biosynthesis of riboflavin. Characterization of the product of the deaminase. *Biochim. Biophys. A.* **662**, 312–317.
9. Richter, G., Fischer, M., Krieger, C., Eberhardt, S., Lüttgen, H., Gerstenschläger, I. & Bacher, A. (1997) Biosynthesis of riboflavin. Characterization of the bifunctional deaminase/reductase of *Escherichia coli* and *Bacillus subtilis*. *J. Bacteriol.* **179**, 2022–2028.
10. Braden, B.C., Vekilovsky, C.A., Cauerhff, A.A., Polikarpov, I. & Goldbaum, F.A. (2000) Divergence in macromolecular assembly: X-ray crystallographic structure analysis of lumazine synthase from *Brucella abortus*. *J. Mol. Biol.* **297**, 1031–1036.
11. Gerhardt, S., Haase, I., Steinbacher, S., Kaiser, J.T., Cushman, M., Bacher, A., Huber, R. & Fischer, M. (2002) The structural basis of riboflavin binding to *Schizosaccharomyces pombe* 6,7-dimethyl-8-ribityllumazine synthase. *J. Mol. Biol.* **318**, 1317–1329.
12. Ladenstein, R., Schneider, M., Huber, R., Bartunik, H.D., Wilson, K., Schott, K. & Bacher, A. (1988) Heavy riboflavin synthase from *Bacillus subtilis*. Crystal structure analysis of the icosahedral β_{60} capsid at 3.3 Å resolution. *J. Mol. Biol.* **203**, 1045–1070.
13. Meining, W., Mörtl, S., Fischer, M., Cushman, M., Bacher, A. & Ladenstein, R. (2000) The atomic structure of pentameric lumazine synthase from *Saccharomyces cerevisiae* at 1.85 Å resolution reveals the binding mode of a phosphonate intermediate analogue. *J. Mol. Biol.* **299**, 181–197.
14. Mörtl, S., Fischer, M., Richter, G., Tack, J., Weinkauf, S. & Bacher, A. (1996) Biosynthesis of riboflavin. Lumazine synthase of *Escherichia coli*. *J. Biol. Chem.* **271**, 33201–33207.
15. Persson, K., Schneider, G., Douglas, B.J., Viitanen, P.V. & Sandalova, T. (1999) Crystal structure analysis of a pentameric fungal and icosahedral plant lumazine synthase reveals the structural basis of diferences in assembly. *Protein Sci.* **8**, 2355–2365.
16. Ritsert, K., Huber, R., Turk, D., Ladenstein, R., Schmidt-Bäse, K. & Bacher, A. (1995) Studies on the lumazine synthase/riboflavin synthase complex of *Bacillus subtilis*: crystal structure analysis of reconstituted, icosahedral beta-subunit capsids with bound substrate analogue inhibitor at 2.4 Å resolution. *J. Mol. Biol.* **253**, 151–167.
17. Zhang, X., Meining, W., Fischer, M., Bacher, A. & Ladenstein, R. (2001) X-ray structure analysis and crystallographic refinements of lumazine synthase from the hyperthermophile *Aquifex aeolicus* at 1.6 Å resolution: determinants of thermostability revealed from structural comparisons. *J. Mol. Biol.* **306**, 1099–1114.
18. Volk, R. & Bacher, A. (1988) Biosynthesis of riboflavin. The structure of the four-carbon precursor. *J. Am. Chem. Soc.* **110**, 3651–3653.
19. Volk, R. & Bacher, A. (1990) Studies on the 4-carbon precursor in the biosynthesis of riboflavin. Purification and properties of L-3,4-dihydroxy-2-butanone 4-phosphate synthase. *J. Biol. Chem.* **265**, 19479–19485.
20. Herz, S., Kis, K., Bacher, A. & Rohdich, F. (2002) A tomato enzyme catalyzing the phosphorylation of 3,4-dihydroxy-2-butanone. *Phytochemistry* **60**, 3–11.
21. Plaut, G.W.E. (1960) Studies on the stoichiometry of the enzymatic conversion of 6,7 dimethyl-8-ribityllumazine to riboflavin. *J. Biol. Chem.* **235**, 41–42.
22. Plaut, G.W.E. (1963) Studies on the nature of the enzymmatic conversion of 6,7-dimethyl-8-ribityllumazine to riboflavin. *J. Biol. Chem.* **238**, 2225–2243.
23. Plaut, G.W.E., Beach, R.L. & Aogaichi, T. (1970) Studies on the mechanismus of elimination of protons from the metyl groups of 6,7-dimethyl-8-ribityllumazine by riboflavin synthetase. *Biochemistry* **9**, 771–785.
24. Plaut, G.W.E. & Harvey, R.A. (1971) The enzymatic synthesis of riboflavin. *Methods Enzymol.* **18**, 515–538.
25. Wacker, H., Harvey, R.A., Winestock, C.H. & Plaut, G.W.E. (1964) 4-(1′-D-Ribitylamino) -5-amino-2,6,-dihydroxypyrimidine, the second product of the riboflavin synthetase reaction. *J. Biol. Chem.* **239**, 3493–3497.
26. Illarionov, B., Eisenreich, W. & Bacher, A. (2001) A pentacyclic reaction intermediate of riboflavin synthase. *Proc. Natl. Acad. Sci. USA* **98**, 7224–7229.
27. Eisenreich, W., Schwarzkopf, B. & Bacher, A. (1991) Biosynthesis of nucleotides, flavins, and deazaflavins in *Methanobacterium thermoautotrophicum*. *J. Mol. Biol.* **266**, 9622–9631.
28. Eberhardt, S., Korn, S., Lottspeich, F. & Bacher, A. (1997) Biosynthesis of riboflavin: an unusual riboflavin synthase of *Methanobacterium thermoautotrophicum*. *J. Bacteriol.* **179**, 2938–2943.
29. Graupner, M., Xu, H. & White, R.H. (2002) The pyrimidine nucleotide reductase step in riboflavin and F (420) biosynthesis in Archaea proceeds by the eukaryotic route to riboflavin. *J. Bacteriol.* **184**, 1952–1957.
30. Sedlmaier, H., Müller, F., Keller, P.J. & Bacher, A. (1987) Enzymatic synthesis of riboflavin and FMN specifically labeled with ^{13}C in the xylene ring. *Z. Naturforsch. C*, **42**, 425–429.
31. Cresswell, R.M. & Wood, H.C.S. (1960) The biosynthesis of pteridines. I. The synthesis of riboflavine. *J. Chem. Soc.*, 4768–4775.

32. Bacher, A. (1986) Heavy riboflavin synthase from *Bacillus subtilis*. *Meth. Enzymol.* **122**, 192–199.
33. Richter, G., Volk, R., Krieger, C., Lahm, H.W., Röthlisberger, U. & Bacher, A. (1992) Biosynthesis of riboflavin: cloning, sequencing, and expression of the gene coding for 3,4-dihydroxy-2-butanone 4-phosphate synthase of *Escherichia coli*. *J. Bacteriol.* **174**, 4050–4056.
34. Stüber, D., Matile, H. & Garotta, G. (1990) System for high level production in *E. coli* and rapid purification of recombinant proteins: application to epitope mapping, preparation of antibodies and structure function analysis. In *Immunological Methods, IV* (Lefkovits, I. & Pernis, P., eds), pp. 121–152.
35. Bullock, W.O., Fernandez, J.M. & Short, J.M. (1987) XL-blue: a high efficiency plasmid transforming recA *Escherichia coli* strain with β-galactosidase selection. *Biotechniques* **5**, 376–379.
36. Braun, N., Tack, J., Fischer, M., Bacher, A., Bachmann, L. & Weinkauf, S. (2000) Electron microscopic observations on protein crystallization: adsorption layers, aggregates and crystal defects. *J. Cryst. Growth* **212**, 270–282.
37. Sanger, F., Niklen, S. & Coulson, A.R. (1977) DNA sequencing with chain-terminating inhibitors. *Proc. Natl. Acad. Sci. USA* **74**, 5463–5467.
38. Schramek, N., Haase, I., Fischer, M. & Bacher, A. (2002) Biosynthesis of riboflavin. Single turnover kinetic analysis of 6,7-dimethyl-8-ribityl-lumazine synthase. *J. Am. Chem. Soc.*, in press.
39. Laemmli, U.K. (1970) Cleavage of structural proteins during the assembly of the head of bacteriophage T4. *Nature* **227**, 680–685.
40. Laue, T. M., Shah, B. D., Ridgeway, T. M. & Pelletier, S. L. (1992) Computer-aided interpretation of analytical sedimentation data for proteins. In *Analytical Ultracentrifugation in Biochemistry and Polymer Science* (Harding, S.E., Rowe, A.J. & Horton, J.C., eds), pp. 90–125, Royal Society of Chemistry, Cambridge.
41. Mann, M. & Wilm, M. (1995) Electrospray mass spectrometry for protein characterization. *Trends Biochem. Sci.* **20**, 219–224.
42. Kis, K., Kugelbrey, K. & Bacher, A. (2001) Biosynthesis of riboflavin. The reaction catalyzed by 6,7-dimethyl-8-ribityllumazine synthase can proceed without enzymatic catalysis under physiological conditions. *J. Org. Chem.* **66**, 2555–2559.
43. Ladenstein, R., Meyer, B., Huber, R., Labischinski, H., Bartels, K., Bartunik, H.D., Bachmann, L., Ludwig, H.C. & Bacher, A. (1984) Electron microscopy and X-ray diffraction studies on heavy riboflavin synthase from *Bacillus subtilis*. In *Flavins and Flavoproteins* (Bray, R.C., Engel, P.C. & Mayhew, S.G., eds), pp 375–378. Walter de Gruyter Verlag, Berlin, Germany.
44. Ladenstein, R., Ludwig, H.C. & Bacher, A. (1983) Crystallization and preliminary X-ray diffraction study of heavy riboflavin synthase from *Bacillus subtilis*. *J. Biol. Chem.* **258**, 11981–11983.
45. Ladenstein, R., Ritsert, K., Huber, R., Richter, G. & Bacher, A. (1994) The lumazine synthase/riboflavin synthase complex of *Bacillus subtilis*. X-ray structure analysis of hollow reconstituted beta-subunit capsids. *Eur. J. Biochem.* **223**, 1007–1017.
46. Kis, K. & Bacher, A. (1995) Substrate channeling in the lumazine synthase/riboflavin synthase complex of *Bacillus subtilis*. *J. Biol. Chem.* **270**, 16788–16795.
47. Kis, K., Volk, R. & Bacher, A. (1995) Biosynthesis of riboflavin. Studies on the reaction mechanism of 6,7-dimethyl-8-ribityl-lumazine synthase. *Biochemistry* **34**, 2883–2892.
48. Fischer, M., Haase, I., Feicht, R., Richter, G., Gerhardt, S., Changeux, J.P., Huber, R. & Bacher, A. (2002) Biosynthesis of riboflavin. 6,7-Dimethyl-8-ribityllumazine synthase of *Schizosaccharomyces pombe*. *Eur. J. Biochem.* **269**, 519–526.
49. Jordan, D.B., Bacot, K.O., Carlson, T.J., Kessel, M. & Viitanen, P.V. (1999) Plant riboflavin biosynthesis. Cloning, chloroplast localization, expression, purification, and partial characterization of spinach lumazine synthase. *J. Biol. Chem.* **274**, 22114–22121.
50. Fischer, M., Haase, I., Kis, K., Meining, W., Ladenstein, R., Schramek, N., Huber, R. & Bacher, A. (2003) Enzyme catalysis via control of activation entropy. Site directed mutagenesis of 6,7-dimethyl-8-ribityllumazine synthase. *J. Mol. Biol.* **326**, 783–793.
51. Zheng, Y.J., Viitanen, P.V. & Jordan, D.B. (2000) Rate limitations in the lumazine synthase mechanism. *Bioorg. Chem.* **27**, 89–97.